Comparative analysis of 5G patch antenna sparse structures characteristics at different frequencies

Manh Tuan Nguyen
Department of Television and Control
Tomsk State University of Control Systems and Radioelectronics
Tomsk, Russia
nguyen.t.2213-2022@e.tusur.ru

Adnan F. Alhaj Hasan
Department of Television and Control
Tomsk State University of Control Systems and Radioelectronics
Tomsk, Russia
alkhadzh@tusur.ru

Talgat R. Gazizov
Department of Television and Control
Tomsk State University of Control Systems and Radioelectronics
Tomsk, Russia
talgat.r.gazizov@tusur.ru

***Abstract*— The integration of antennas into the urban environment without compromising the overall landscape is a significant challenge at present. One effective solution is to sparse wire grid antennas to create structures that can be integrated into different environments. The Optimal Current Grid Approximation approach and its modifications allow the creation of structures with smaller mass than traditional ones, while maintaining the required performance. However, the difference in the current distribution in the original wire grid leads to obtain different sparse structures at different frequencies after applying these approaches. This study focuses on analyzing and comparing the performance of sparse patch antenna structures obtained at different frequencies in the operating frequency range. Frequencies of 2, 2.6 and 3 GHz are chosen to generate these sparse structures. The characteristics of these sparse structures are compared with each other and with those of the original one. The advantages and disadvantages of each structure are discussed. Proper recommendations are given for selecting which approach to use as well as the frequency at which the sparse structure can be generated. In addition, this study compares the characteristics of different sparse structures over the operating frequency range to help manufacturers select a sparse structure that fulfills specific requirements.**

Keywords—wire-grid, sparse antennas, 3D printing, patch antennas, method of moments, optimal current grid approximation, 5G networks, hidden antenna.

I. INTRODUCTION

In today's technological era, wireless communication has become an essential part of urban life. With the rapid development of Smart City and 5G networks, the need for efficient and flexible antennas becomes even more important [1, 2]. One of the most advanced types of antennas that satisfy these demands are patch antennas. They are widely used in Internet of Things (IoT) and Smart City applications [3–5]. However, their designs that operate at high frequencies often experience difficulties in maintaining performance and minimizing losses. This requires advanced design techniques and the use of new materials to improve their performance. Moreover, integrating large patch antennas into urban environments is also challenging.

To overcome these challenges, researchers have considered many design techniques, including the use of wire grid (WG) to approximate the metal surface of the patch antenna [6–8]. The WG structure consists of electrically interconnected wires that form a grid with different cell shapes. The equivalent WG structure reduces the mass of the patch antenna by using less material than traditional designs. At the same time, the fabrication of WG structures can be done at a lower cost, especially when using advanced manufacturing technologies such as 3D printing [9–11]. This makes WG patch antennas a budget-friendly and efficient choice for many applications.

In urban environments where space is limited and high aesthetics are required, antennas must be optimized in both performance and size to meet these requirements. Researchers have presented many new techniques to develop new types of antennas to address this issue [12–14]. One of them is to utilize sparse antennas by replacing their conventional structures with ones of lower mass while maintaining the required performance [15–17]. To generate sparse structures, the Optimal Current Grid Approximation (OCGA) WG-based approach has recently received much attention. OCGA was first proposed in [18]. It can generate a sparse WG structure consisting only of wires following the current path. Sparse structures are created by excluding wires whose normalized current magnitude is less than a given threshold. This threshold value is called the Grid Element Elimination Tolerance (GEET). Depending on the original WG structure type, the current magnitude in each WG wire can be normalized to the maximum or average current magnitude of all wires. Further, the GEET value can be adjusted to establish sparse structures that satisfy specific requirements. However, as the GEET value increases, unconnected (free) wires to the WG structure increasingly appear. This leads to discontinuity in the grid electrical paths, making it difficult to fabricate the WG antenna. Therefore, two modifications of OCGA were proposed in [19] to deal with this problem namely “eliminating” OCGA (EOCGA) and “near-connecting” OCGA (NCOCGA). The principle of the EOCGA approach is to eliminate all free wires, while NCOCGA is to rebuild only the necessary wires to reconnect the free ones to the structure.

In [20], a WG patch antenna for a 5G network was modeled using various computer-aided design systems. The simulation results obtained by different numerical methods are compared with each other and with the measured results for the antenna model fabricated using the 3D printing technique in [21]. The calculation results of the WG structure obtained using MoM with pulse basis functions in TALGAT [22] showed good agreement with the experimental ones. Consequently, this WG was chosen as the original structure to apply OCGA, EOCGA and NCOCGA approaches on it.

The sparse structures generated based on the WG current distribution obtained at the center frequency were considered and analyzed. However, the current distribution in the WG structure is known to be different when calculated at different frequencies in the considered frequency range. This has a direct effect on the resulting sparse structures. To investigate this influence, it is necessary to analyze the

This research was funded by the Ministry of Science and Higher Education of the Russian Federation project FEWM-2023-0014.

sparse structures obtained at different frequencies in the operating frequency range. Therefore, the aim of this paper is to comparatively analyze the performance of sparse patch antennas obtained after applying OCGA and its modifications at different frequencies in the operating range, and to provide guidelines for selecting the frequency at which sparse structures can be created with acceptable performance, as well as the suitable approach for this purpose.

This study is organized as follows: Section II presents the GEET dependence of the sparse antenna structures after applying OCGA and its modifications based on the WG current distribution at different frequencies in the antenna operating range. This section also provides a comparative analysis of the performance of each sparse structure compared to the original WG followed by a discussion of their merits and demerits. Section III shows the sparse antennas obtained after applying different approaches with specific GEET values. Furthermore, it analyzes their characteristics with respect to those of the original WG in the operating frequency range. Section IV summarizes the results of the study and draws conclusions based on the conducted analyses.

II. GEET Dependences of Sparse Antenna Characteristics

A substrateless WG patch antenna from [21] is considered in this study. Its structure is designed to operate at a center frequency of 2.6 GHz in the frequency range of 2–3 GHz, and its geometrical parameters are well detailed in [21]. OCGA and its modifications are applied to generate equivalent sparse WG structures at the center and boundary frequencies of 2 and 3 GHz. These structures are shown in Fig. 1 where it is also demonstrated that the current distribution in them at the considered frequencies is different. It can be seen that the highest current module is obtained at the center frequency (0.0224 A), while smaller modules are obtained at the boundary ones (0.00433 A and 0.00791 A).

To avoid confusion, the sparse structures obtained at 2, 2.6, and 3 GHz are denoted as S_2, $S_{2.6}$, and S_3, respectively. By varying the GEET value, the number of remaining wires in the WG structure also varies after applying different approaches to different structures. The dependencies of the total number of remaining wires on GEET when changing its value from 0 to 50% are shown in Fig. 2. When this number is changed, it directly affects the antenna mass and the time and memory required for its subsequent simulations. Their GEET dependences are shown in Fig. 3.

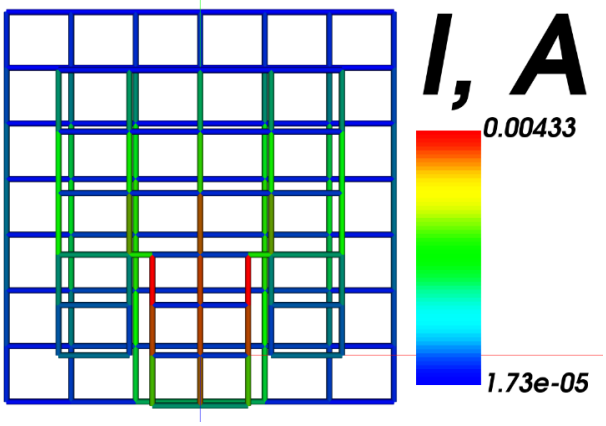

(*a*)

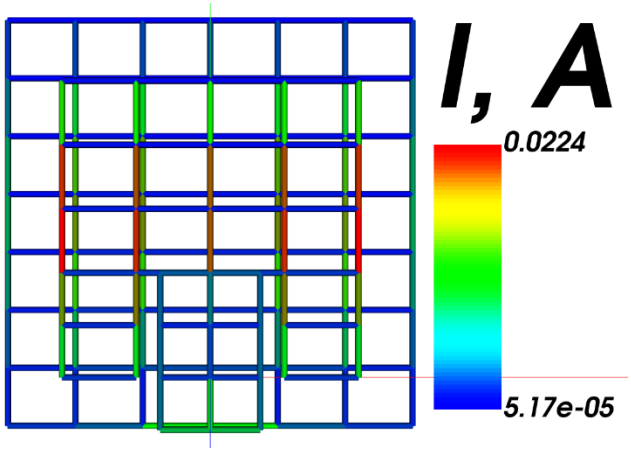

(*b*)

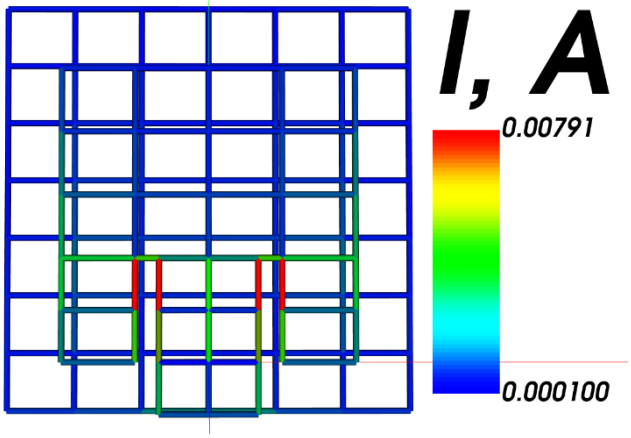

(*c*)

Fig. 1. Current distribution in the original WG structure at frequencies of 2 (*a*), 2.6 (*b*) and 3 (*c*) GHz.

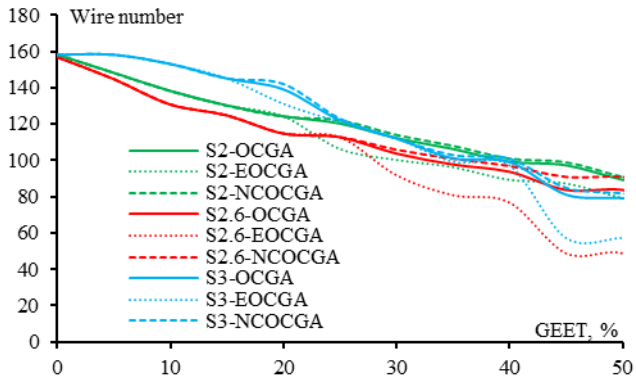

Fig. 2. GEET dependencies of the total number of remaining wires after OCGA, EOCGA and NCOCGA for S_2, $S_{2.6}$ and S_3.

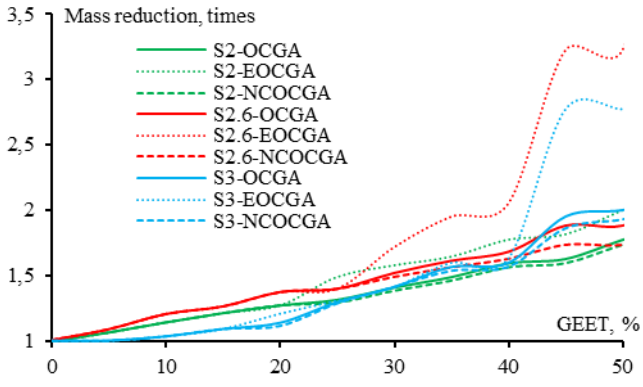

(*a*)

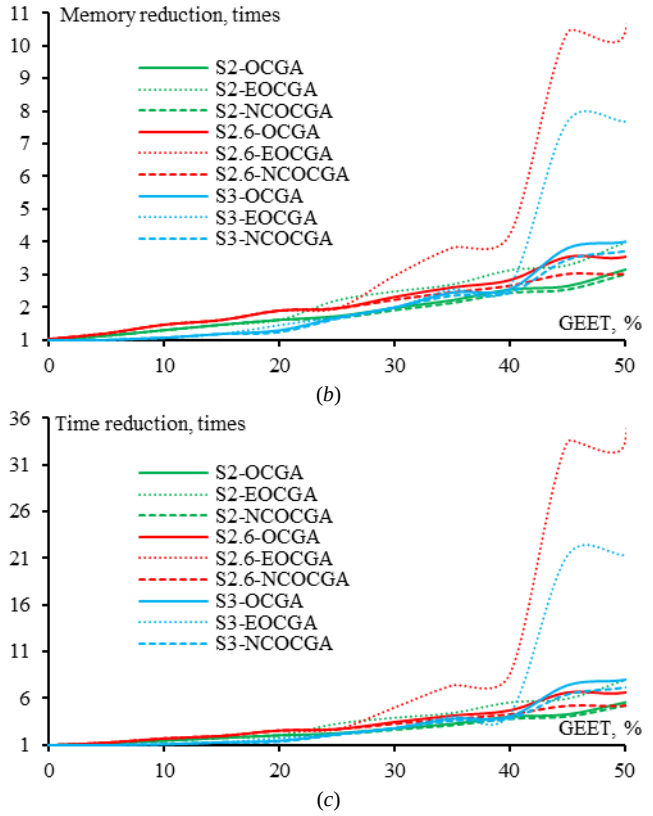

Fig. 3. GEET dependences of the reduction in the antenna mass (*a*), and required memory (*b*) and time (*c*) for further simulations after OCGA, EOCGA and NCOCGA for S_2, $S_{2.6}$ and S_3.

The results in Fig. 2 show that the number of remaining wires in the sparse structure $S_{2.6}$ is generally smaller than that in S_2 and S_3. When GEET<25%, the number of remaining wires in S_3 is significantly larger than that in $S_{2.6}$ and S_2, and when GEET>25%, these numbers become closer. This leads to the fact that the reduction in mass as well as memory and time for subsequent simulations for the $S_{2.6}$ structure is basically higher than for the other structures. Furthermore, when comparing the considered approaches, it is observed that the sparse structure obtained after EOCGA always has the least number of remaining wires, followed by OCGA and NCOCGA. This can be explained by the fact that NCOCGA restores some of the wires required to establish connections between the free wires and the structure, while EOCGA eliminates them.

Changes in the obtained WG sparse structures directly affect their characteristics. To analyze this influence, the dependences of the antenna characteristics such as the maximum gain (G_{max}), voltage standing wave ratio (VSWR), reflection coefficient magnitude $|S_{11}|$ and input impedance magnitude $|Z|$ obtained for different sparse structures on GEET are examined and compared with their values for the original WG structure (when GEET=0%) at different frequencies (summarized in Table I). The characteristics of S_2, $S_{2.6}$ and S_3 obtained by changing GEET from 0 to 50% at frequencies 2, 2.6 and 3 GHz are presented in Figs. 4–6, respectively. Their maximum differences from those of the original WG are listed in Table II. These findings allow manufacturers to choose the most suitable approach and frequency at which the sparse structure should be created.

By comparing all antenna characteristics, it can be seen that structure S_2 at 2 GHz gives stable results and is less affected by the GEET value compared to other structures. The results in Table II also show that most of the smallest values of maximum differences from the original structure at a considered frequency are obtained for its corresponding structure generated at it, e.g. structure S_2 at 2 GHz, $S_{2.6}$ at 2.6 GHz (values in italics in Table II). The difference in characteristics of these structures from those of the original one is practically insignificant at GEET<25%, and at GEET>25% it becomes more noticeable. Considering the difference at different frequencies for the same sparse structure (bold values in Table II), it can be observed that the results of G_{max} and $|S_{11}|$ differ minimally at the center frequency of 2.6 GHz, while VSWR –at 3 GHz, and $|Z|$ –at frequencies corresponding to the frequency at which the sparse structure is created.

TABLE I. ORIGINAL WG STRUCTURE ANTENNA CHARACTERISTICS AT THE CONSIDERED FREQUENCIES

f, GHz	G_{max}, dB	VSWR	$\|S_{11}\|$, dB	$\|Z\|$, Ohm
2	10.87	225.64	-0.08	517.73
2.6	11.14	3.16	-5.69	77.98
3	4.95	39.47	-0.44	448.16

TABLE II. COMPARING PATCH ANTENNA SPARSE STRUCTURES CHARACTERISTICS WITH THOSE OF ITS ORIGINAL STRUCTURE

f, GHz	Sparse Structures		Maximum Difference, %			
			G_{max}	VSWR	$\|S_{11}\|$	$\|Z\|$
2	S_2	OCGA	*27.19*	*84.70*	*271.67*	***21.74***
		EOCGA	*20.22*	*93.86*	*119.39*	***21.85***
		NCOCGA	*30.91*	*75.54*	***43.03***	***22.35***
	$S_{2.6}$	OCGA	41.53	93.06	1343.51	222.52
		EOCGA	49.47	95.97	2393.09	117.59
		NCOCGA	33.25	96.59	2849.61	107.91
	S_3	OCGA	43.90	137.98	3301.38	58.43
		EOCGA	45.57	137.74	3446.10	60.43
		NCOCGA	39.09	238.89	983.47	48.99
2.6	S_2	OCGA	**10.19**	720.68	**88.23**	140.72
		EOCGA	***6.75***	531.85	**84.70**	132.70
		NCOCGA	**9.91**	684.33	87.68	134.86
	$S_{2.6}$	OCGA	***10.06***	***34.02***	***59.45***	***68.54***
		EOCGA	**40.72**	*196.24*	**173.91**	***31.39***
		NCOCGA	***2.89***	*169.33*	***67.31***	***44.31***
	S_3	OCGA	**40.87**	391.73	**80.33**	795.85
		EOCGA	**43.48**	372.85	***83.00***	833.97
		NCOCGA	**24.37**	349.22	**78.47**	299.82
3	S_2	OCGA	30.44	***49.99***	*100.07*	47.93
		EOCGA	*30.44*	***49.99***	*100.07*	47.58
		NCOCGA	82.20	**70.44**	239.06	45.68
	$S_{2.6}$	OCGA	*24.77*	83.52	511.48	94.94
		EOCGA	66.60	**86.66**	658.69	93.65
		NCOCGA	*24.77*	**68.25**	215.61	81.28
	S_3	OCGA	50.83	**67.49**	208.14	***22.52***
		EOCGA	47.47	**67.02**	203.73	***22.87***
		NCOCGA	44.43	***46.93***	*88.55*	***11.94***

Comparison of the results obtained after applying OCGA, EOCGA and NCOCG shows small differences at low GEET values, which become more noticeable as GEET increases. This can be explained by the appearance of free wires at high GEET values. Table II shows that the smallest differences are most often observed after applying NCOCGA at the main frequencies (underlined values in Table II). In particular, the number of smallest maximum differences after applying NCOCGA is 7, while after OCGA – 4 and after EOCGA – 2. In addition, when comparing the results at all frequencies with each other, the smallest maximum differences in G_{max}, $|S_{11}|$ and $|Z|$ are obtained after NCOCGA, while in VSWR – after OCGA (values highlighted in red in Table. II).

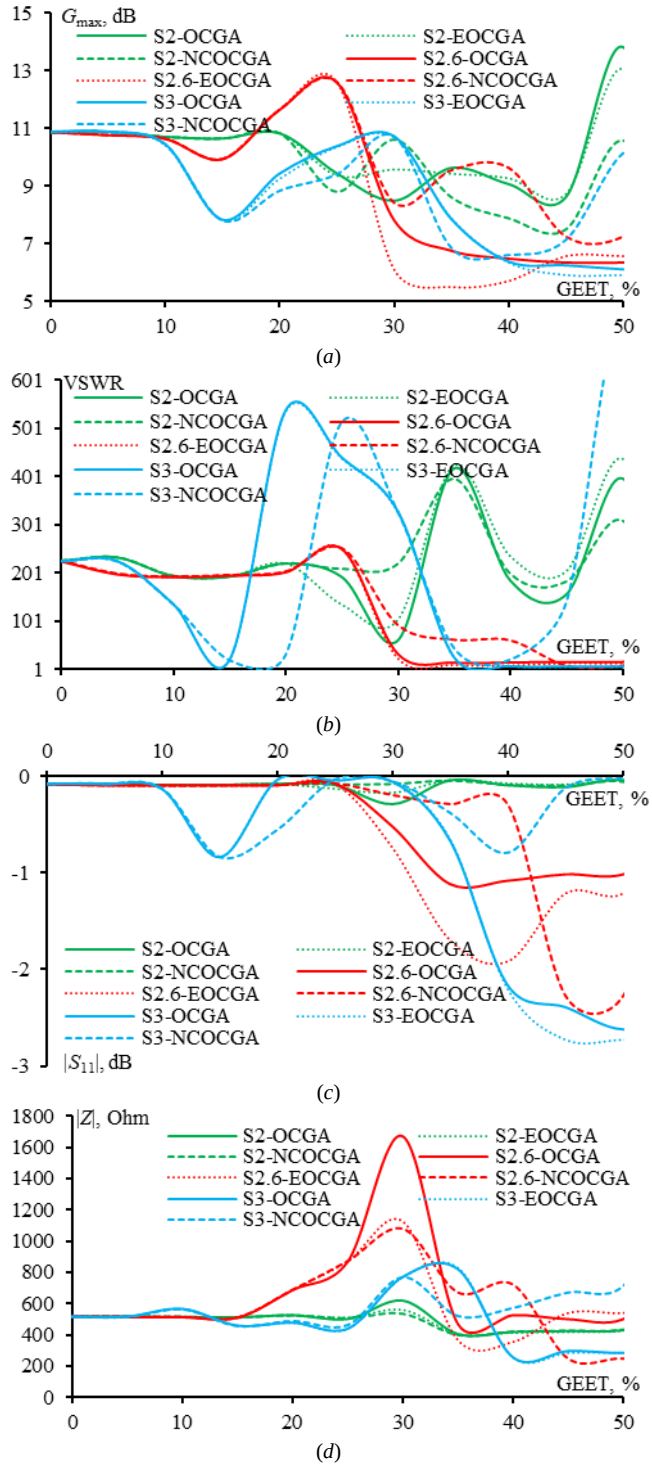

Fig. 4. GEET dependences of G_{max} (*a*), VSWR (*b*), $|S_{11}|$ (*c*), and $|Z|$ (*d*) after OCGA, EOCGA and NCOCGA for S_2, $S_{2.6}$ and S_3 at 2 GHz.

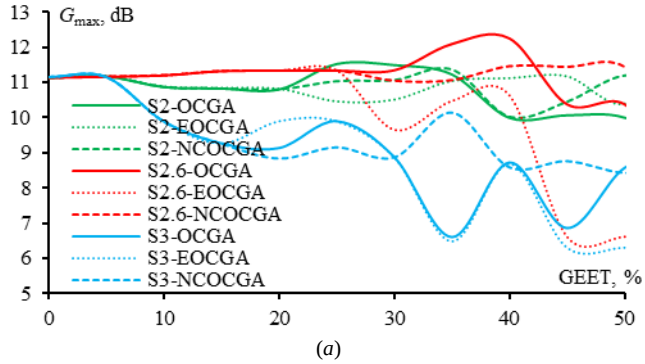

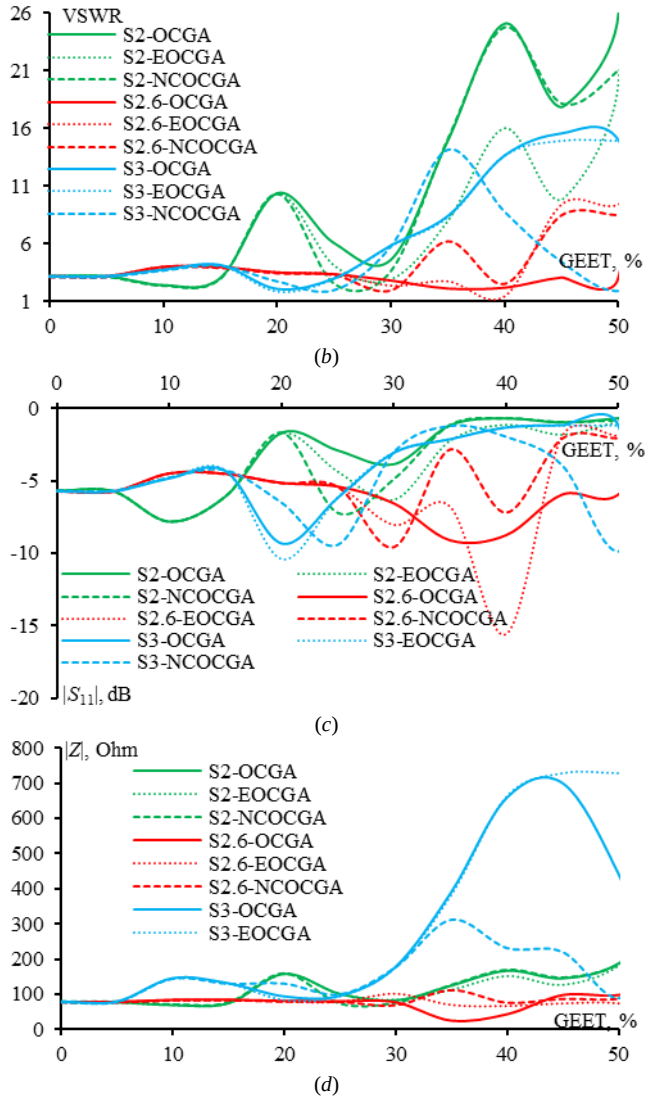

Fig. 5. GEET dependences of G_{max} (*a*), VSWR (*b*), $|S_{11}|$ (*c*), and $|Z|$ (*d*) after OCGA, EOCGA and NCOCGA for S_2, $S_{2.6}$ and S_3 at 2.6 GHz.

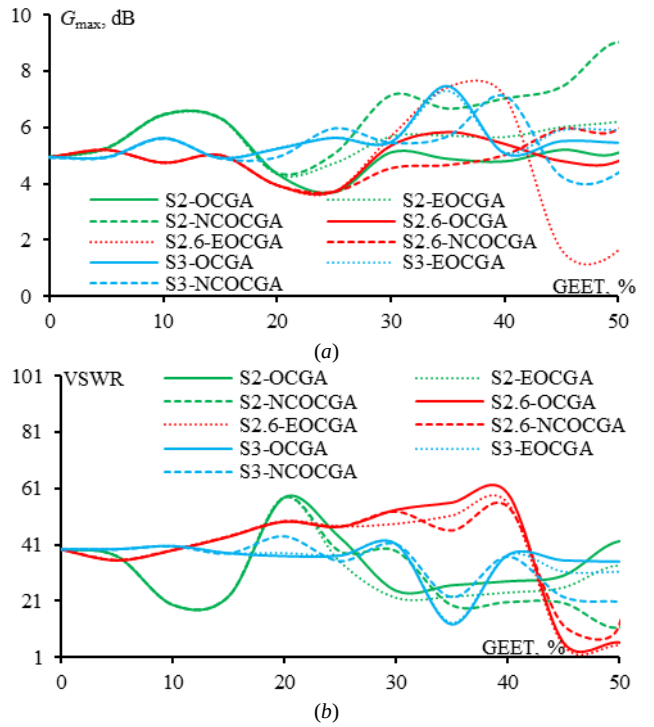

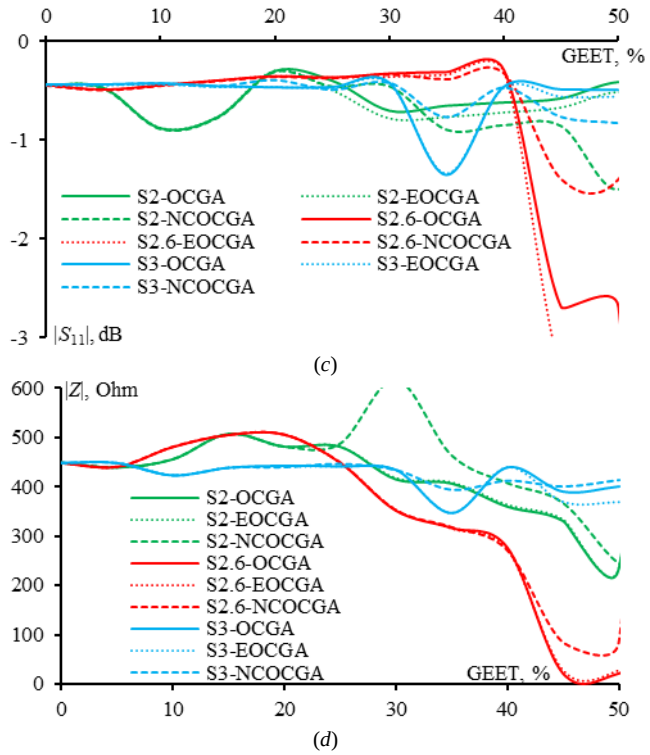

Fig. 6. GEET dependences of G_{max} (*a*), VSWR (*b*), $|S_{11}|$ (*c*), and $|Z|$ (*d*) after OCGA, EOCGA and NCOCGA for S_2, $S_{2.6}$ and S_3 at 3 GHz.

This demonstrates that NCOCGA provides higher accuracy and preserves the original antenna characteristics more than OCGA and EOCGA. NCOCGA maintains a seamless WG structure without interrupting the current path. However, compared to OCGA and EOCGA, NCOCGA gives sparse antenna with larger mass and more required computational costs for its further simulations. Therefore, manufacturers should carefully evaluate their requirements before selecting the most appropriate approach among the considered ones.

III. Sparse Antenna Characteristics at Specific GEETs

To analyze the characteristics of the sparse antennas obtained in the operating frequency range, examples of sparse structures obtained after applying different approaches with GEET=30% are provided in this section. The sparse structures S_2, $S_{2.6}$ and S_3 obtained after applying OCGA, EOCGA and NCOCGA with the same value of GEET=30% are shown in Fig. 7. Analyzing the obtained sparse structures, it can be noticed that some free wires appeared in the sparse structures S_2 and $S_{2.6}$ obtained after OCGA (Fig. 7*a*, *d*), thus EOCGA removed these wires (Fig. 7*b*, *e*), while NCOCGA restored those wires necessary to create connections between these free wires and the structure (Fig. 7*c*, *f*). The sparse S_3 structure has no free wires after OCGA, so similar sparse structures are obtained after EOCGA and NCOCGA. This demonstrates the ability of EOCGA and NCOCGA to accurately identify free wires and remove them or restore those needed for the connection. In addition, it can be noticed that the numbers of remaining wires in the WG structures are not the same, resulting in different reductions in antenna mass, memory and time required for subsequent simulations for each sparse structure. The numbers of remaining wires in these structures as well as the reductions obtained thanks to them are listed in Table III.

TABLE III. Total Numbers of Remaining Wires in the Sparse Structures and their Improvements Relative to the Original One

Sparse structures		Remaining wires	Reduction, times		
			Mass	Memory	Time
S_2	OCGA	112	1.41	1.99	2.81
	EOCGA	100	1.58	2.50	3.94
	NCOCGA	114	1.39	1.92	2.66
$S_{2.6}$	OCGA	104	1.52	2.31	3.51
	EOCGA	92	1.72	2.95	5.07
	NCOCGA	106	1.49	2.22	3.31
S_3	OCGA	112	1.41	1.99	2.81
	EOCGA	112	1.41	1.99	2.81
	NCOCGA	112	1.41	1.99	2.81

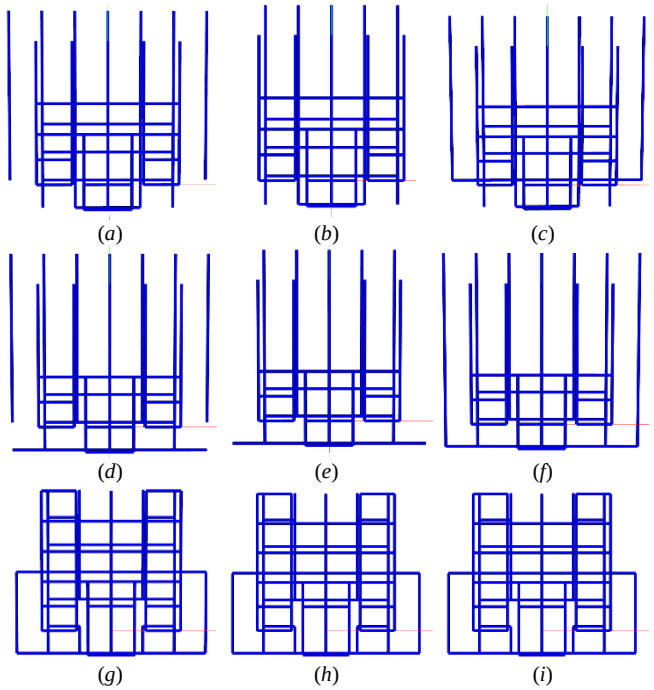

Fig. 7. Sparse WG structures after OCGA, EOCGA and NCOCGA at GEET=30%: S_2 (*a*, *b*, *c*), $S_{2.6}$ (*d*, *e*, *f*) and S_3 (*g*, *h*, *i*) respectively

The results in Table III show that the number of remaining wires in the sparse structure $S_{2.6}$ is the smallest after applying different approaches. This means that for this structure the reductions in antenna mass as well as in modeling costs are higher compared to other structures. However, it is also important to analyze the characteristics of these different sparse structures in the frequency range. Therefore, the characteristics of S_2, $S_{2.6}$ and S_3 such as G_{max}, VSWR, $|S_{11}|$ and $|Z|$ are compared with each other and with those of the original WG structure in the frequency range of 2.5–2.7 GHz (Fig. 8). The maximum differences in the sparse antenna characteristics compared to those of the original WG in this frequency range are listed in Table IV.

TABLE IV. Maximum Differences of Sparse Antenna Characteristics Compared to the Original WG in 2.5–2.7 GHz

Sparse structures		Maximum Difference			
		G_{max}, dB	VSWR	$\|S_{11}\|$, dB	$\|Z\|$, Ohm
S_2	OCGA	1.81	4.73	7.73	**29.27**
	EOCGA	**1.14**	**4.61**	**11.01**	**35.49**
	NCOCGA	**0.34**	3.50	**6.97**	**9.36**
$S_{2.6}$	OCGA	**0.22**	**2.79**	**6.04**	41.49
	EOCGA	1.54	11.52	15.88	66.63
	NCOCGA	0.88	**3.08**	15.81	136.12
S_3	OCGA	2.42	17.88	22.63	293.76
	EOCGA	2.42	17.88	22.63	293.76
	NCOCGA	2.42	17.88	22.63	293.76

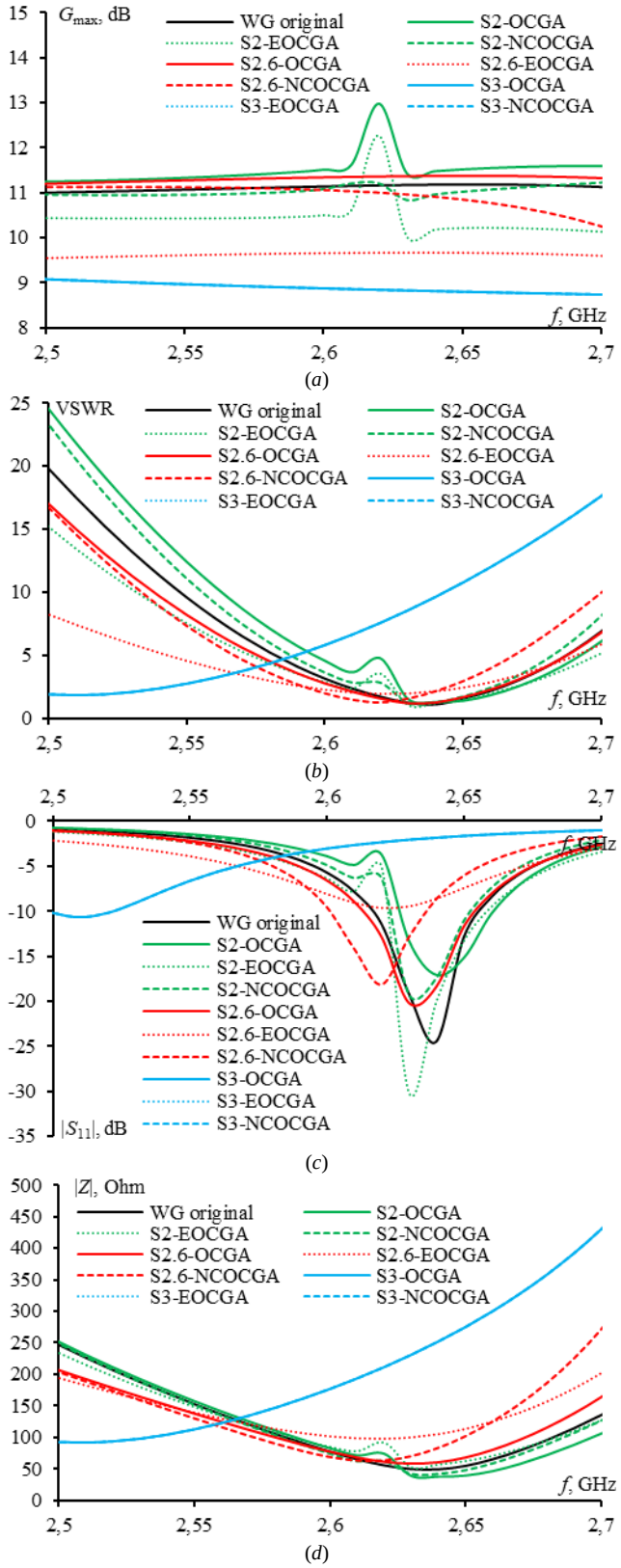

Fig. 8. Frequency dependencies of the obtained G_{max} (*a*), VSWR (*b*), $|S_{11}|$ (*c*), and $|Z|$ (*d*) of the original and sparse WG antennas after OCGA, EOCGA and NCOCGA for S_2, $S_{2.6}$ and S_3 at GEET=30%.

Furthermore, the radiation patterns (RPs) for different sparse WG structures after all considered approaches and at the center frequency of 2.6 GHz in the *E* and *H* planes are obtained. These RPs are compared with each other and with those obtained for the original WG and demonstrated in Fig. 9.

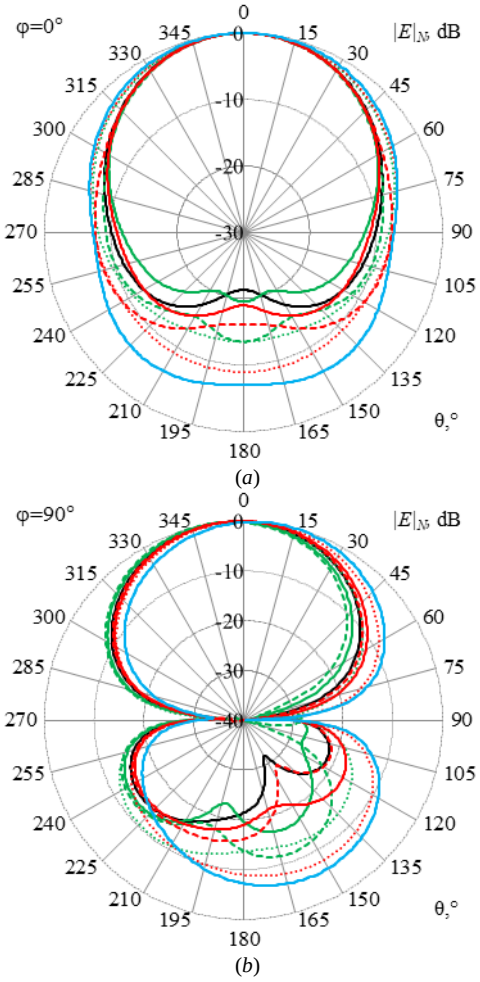

Fig. 9. Obtained RPs in *E* (*a*) and *H* (*b*) planes at 2.6 GHz for the original (—) and sparse S_2-OCGA (—), S_2-EOCGA (····), S_2-NCOCGA (- -), $S_{2.6}$-OCGA (—), $S_{2.6}$-EOCGA (····), $S_{2.6}$-NCOCGA (- -), S_3-OCGA (—), S_3-EOCGA (····), S_3-NCOCGA (- -) WG structures.

The results in Fig. 8 show that in the considered frequency range, the S_2 and $S_{2.6}$ sparse structures give results similar to those of the original WG structure, while the results for the S_3 sparse structure have significant differences in both behavior and amplitude. This is also evident from Table IV where the lowest values of maximum differences after applying OCGA, EOCGA and NCOCGA approaches are obtained for S_2 and $S_{2.6}$ structures (bold values in Table IV). Analyzing the maximum difference from the original structure results for all structures after applying different approaches in the considered frequency range (red values in Table IV), its lowest values for G_{max}, VSWR and $|S_{11}|$ are obtained for structure $S_{2.6}$ after OCGA, and for $|Z|$ are obtained for structure S_2 after NCOCGA. The compared RPs in Fig. 9 also show a good agreement for the $S_{2.6}$ structure after OCGA compared to the original one. Comparing the results regarding the considered approaches, it can be noticed that the results obtained after OCGA and NCOCGA have small differences compared to those of the original WG, while the difference is significant after EOCGA. However, this can be considered acceptable if one considers the reduction in antenna mass as well as the costs of subsequent simulations after EOCGA. Thus, it is recommended to generate the sparse structure of the considered patch antenna at the center or, preferably, at low frequencies in its operating range, since they give results close to the original one. In general, the conducted analyses allow manufacturers

to select sparse structure suitable for their requirements. In addition, as it is seen these sparse structures come in a variety of shapes and sizes, allowing them to be easily integrated in urban environments without disturbing the overall landscape and also in small portable devices.

IV. Conclusion

Thus, in this paper, the influence of selecting the frequency at which the sparse structure is created on its characteristics is considered. The current distributions in the original WG structure at specific frequencies were analyzed. Based on them, the OCGA, EOCGA and NCOCGA approaches were applied to generate different sparse structures. The GEET dependence of the antenna characteristics for these structures were compared with each other and with those of the original one at the considered frequencies. Comparisons revealed that a sparse structure generated at a particular frequency gives results that are less affected by changing the GEET value and are closer to those of the original structure at that frequency. They also demonstrated the effectiveness of NCOCGA in generating sparse structures with characteristics more similar to those of the original antenna than other approaches. However, OCGA and EOCGA provide greater reduction in mass and costs required for subsequent simulations using their sparse structures instead of the solid or original WG.

A comparative analysis of sparse WG structures obtained after applying OCGA and its modifications with specific GEET value is carried out. Their characteristics are compared with those of the original structure in the operating frequency range. The analysis revealed that the sparse WG structures generated at low and center frequencies give closer characteristics to those of the original WG. These structures can replace the original WG or the solid structures providing gains in mass and modeling costs. Moreover, they have different shape and size compared to traditional antenna structures. Thus, they can be installed in buildings, lampposts, portable devices and even vehicles to enable connectivity in urban environments without affecting the general landscape due to their high transparency and small size and mass. This study can help manufacturers to select the appropriate approach and frequency at which sparse structures might be created to meet their requirements.

References

[1] S. G. Kirtania et al., “Flexible Antennas: A Review,” Micromachines, vol. 11, no. 9, p. 847, 2020, doi: 10.3390/mi11090847.

[2] A. S. M. Sayem et al., “Flexible Transparent Antennas: Advancements, Challenges, and Prospects,” in IEEE Open Journal of Antennas and Propagation, vol. 3, pp. 1109–1133, 2022, doi: 10.1109/OJAP.2022.3206909.

[3] L. Anchidin et al., “The Design and Development of a Microstrip Antenna for Internet of Things Applications,” Sensors, vol. 23, no. 3, p. 1062, 2023, doi: 10.3390/s23031062.

[4] F. Mahbub et al., “A Single-Band 28.5GHz Rectangular Microstrip Patch Antenna for 5G Communications Technology,” 2021 IEEE 11th Annual Computing and Communication Workshop and Conference (CCWC), NV, USA, 2021, pp. 1151-1156, doi: 10.1109/CCWC51732.2021.9376047.

[5] D. Surender, T. Khan and F. A. Talukdar, “A Triple-band Hexagonal-Shaped Microstrip Patch Antenna for RF Energy Harvesting in Smart City Applications,” 2020 IEEE International Conference on Computing, Power and Communication Technologies (GUCON), Greater Noida, India, 2020, pp. 389–393, doi: 10.1109/GUCON48875.2020.9231228.

[6] S. Hong, Y. Kim and C. Won Jung, “Transparent Microstrip Patch Antennas With Multilayer and Metal-Mesh Films,” in IEEE Antennas and Wireless Propagation Letters, vol. 16, pp. 772–775, 2017, doi: 10.1109/LAWP.2016.2602389.

[7] S. H. Kang and C. W. Jung, “Transparent Patch Antenna Using Metal Mesh,” in IEEE Transactions on Antennas and Propagation, vol. 66, no. 4, pp. 2095–2100, April 2018, doi: 10.1109/TAP.2018.2804622.

[8] P. Duy Tung and C. W. Jung, “Optically Transparent Wideband Dipole and Patch External Antennas Using Metal Mesh for UHD TV Applications,” in IEEE Transactions on Antennas and Propagation, vol. 68, no. 3, pp. 1907–1917, March 2020, doi: 10.1109/TAP.2019.2950077.

[9] M. Liang et al., “3-D Printed Microwave Patch Antenna via Fused Deposition Method and Ultrasonic Wire Mesh Embedding Technique,” in IEEE Antennas and Wireless Propagation Letters, vol. 14, pp. 1346–1349, 2015, doi: 10.1109/LAWP.2015.2405054.

[10] C. M. Shemelya, M. Zemba, C. Kief, D. Espalin, R. B. Wicker and E. MacDonald, “Multi-layer off-axis patch antennas fabricated using polymer extrusion 3D printing,” 2016 10th European Conference on Antennas and Propagation (EuCAP), Davos, Switzerland, 2016, pp. 1–5, doi: 10.1109/EuCAP.2016.7481678.

[11] M. Kacar, T. M. Weller and G. Mumcu, “3D Printed Wideband Multilayered Dual-Polarized Stacked Patch Antenna With Integrated MMIC Switch,” in IEEE Open Journal of Antennas and Propagation, vol. 2, pp. 38–48, 2021, doi: 10.1109/OJAP.2020.3041959.

[12] S. Kumar, A. S. Dixit, R. R. Malekar, H. D. Raut and L. K. Shevada, “Fifth Generation Antennas: A Comprehensive Review of Design and Performance Enhancement Techniques,” in IEEE Access, vol. 8, pp. 163568–163593, 2020, doi: 10.1109/ACCESS.2020.3020952.

[13] N. Ojaroudi Parchin et al., “Reconfigurable Antennas: Switching Techniques–A Survey,” Electronics, vol. 9, no. 2, p. 336, 2020, doi: 10.3390/electronics9020336.

[14] C. Fager et al., “Linearity and Efficiency in 5G Transmitters: New Techniques for Analyzing Efficiency, Linearity, and Linearization in a 5G Active Antenna Transmitter Context,” in IEEE Microwave Magazine, vol. 20, no. 5, pp. 35–49, May 2019, doi: 10.1109/MMM.2019.2898020.

[15] E. Tohidi, et al., “Sparse Antenna and Pulse Placement for Colocated MIMO Radar,” in IEEE Transactions on Signal Processing, vol. 67, no. 3, pp. 579-593, 1 Feb.1, 2019, doi: 10.1109/TSP.2018.2881656.

[16] S. Zhang, S. Zhang, F. Gao, J. Ma and O. A. Dobre, “Deep Learning Optimized Sparse Antenna Activation for Reconfigurable Intelligent Surface Assisted Communication,” in IEEE Transactions on Communications, vol. 69, no. 10, pp. 6691–6705, Oct. 2021, doi: 10.1109/TCOMM.2021.3097726.

[17] E. O. Owoola, K. Xia, T. Wang, A. Umar and R. G. Akindele, “Pattern Synthesis of Uniform and Sparse Linear Antenna Array Using Mayfly Algorithm,” in IEEE Access, vol. 9, pp. 77954–77975, 2021, doi: 10.1109/ACCESS.2021.3083487.

[18] A. Alhaj Hasan, T. M. Nguyen, S. P. Kuksenko and T. R. Gazizov, “Wire-grid and sparse MoM antennas: past evolution, present implementation and future possibilities,” Symmetry, 2023, vol. 15(2), p. 378. doi: 10.3390/sym15020378.

[19] A. A. Hasan, T. M. Nguyen and T. R. Gazizov, “Novel MoM-Based Approaches for Generating Wire-Grid Sparse Antenna Structures," IEEE 24th International Conference of Young Professionals in Electron Devices and Materials (EDM), Novosibirsk, Russia, 2023, pp. 570–576, doi: 10.1109/EDM58354.2023.10225219.

[20] M. T. Nguyen, A. F. Alhaj Hasan and T. R. Gazizov, “Sparse wire grid 3D printed patch antenna,” Wave electronics and its application in information and telecommunication systems, Saint-Petersburg, Russia, 2024. To be published.

[21] Inclán-Sánchez L. “Performance Evaluation of a Low-Cost Semitransparent 3D-Printed Mesh Patch Antenna for Urban Communication Applications” Electronics, vol. 13, no. 1. pp. 153, 2024, doi: 10.3390/electronics13010153.

[22] TALGAT system. Available online: https://talgat.org/talgat-software/ (accessed on 15.05.2024).